Monitoring the properties of the atmosphere relevant for the observation of cosmic rays and cosmic gamma rays with atmospheric Cherenkov telescopes

Amandeep Singh
Supervised by Prof. Dr. Adrian Biland

19th March, 2018

Abstract

Atmospheric Cherenkov telescopes are a great tool for monitoring cosmic rays and cosmic gamma rays with energies above ~100GeV.
However, atmospheric Cherenkov telescopes rely heavily on the atmosphere as a calorimeter. But the atmosphere changes over time, and it's not exactly clear how these changes affect the performance of these telescopes.
We propose here a method to monitor the properties of the atmosphere, using the telescope itself, not using external devices which may hinder the data taking of other nearby instruments by emitting light.
To monitor the atmosphere, we take a look at the structure of the arrival-times (multiplicity) of single photons on the nanosecond level. Here we present correlations of the multiplicity of single photons with ambient and atmospheric properties.

Keywords: Multiplicity, air shower, night sky background, Cherenkov Light, single photons, gamma rays, cosmic rays.

Introduction

Cosmic rays are particles (protons, nuclei of different elements, electrons, etc.) bombarding the earth's atmosphere. Although there are many candidates for the origin of such particles, the exact origin of these particles is unknown. After entering the earth's atmosphere, the particles collide with different air molecules. This collision creates further particles, and those particles collide further, creating more particles, thus creating a cascade of particles that is know as an air shower. The particles seldom reach the ground, but they can be detected using different detection methods. The particles that move faster than the speed of light in the atmosphere (speed of light in vacuum divided by the refractive index of atmosphere), emit a blue hue that can be detected on ground. This blue light is called Cherenkov light[1]. By detecting these Cherenkov photons, we can reconstruct the geometry of the air shower, and hence can learn about the cosmic ray that started the air shower.

FACT (the First G-APD Cherenkov Telescope)-is a small telescope of 4 meter mirror diameter, 4.5 degrees field of view, 1440 pixels, and can record arrival times of individual single photons in the 1 nanosecond regime/level. [2][3] FACT records these Cherenkov photons emitted from the high speed particles. It also records auxiliary data, such as humidity, pressure conditions, atmospheric density in it's direct vicinity, various temperature conditions of the telescope itself, electric bias, etc., and stores them in individual chunks of a period of five-minutes each. We call this five-minute time period a single "run". During this time it is assumed that all these auxiliary conditions remain constant.

Method

We define multiplicity as the number of photons arriving in a dense cluster of photons with respect to time. We are integrating occurrences of multiplicities over all the pixels and over all recorded air showers.

Generally the arrival times of the night-sky-background-photons often follow a Poissonian distribution, and so are not expected to have high multiplicities. On the other hand the arrival times of air shower photons have dense structures, so we expect air showers photons to have high multiplicities.

FACT is recording the incoming directions and the arrival times of individual single photons. The output structure of FACT is a list of arrival times of individual photons in each individual pixel.

For extracting the multiplicities, we use the density-based clustering algorithm DBSCAN [8] in one dimension. DBSCAN works in two steps: (1) first finding the seed for the cluster, (2) then expanding the cluster. So for implementing these steps, it takes in two input parameters: (1) time-radius (which is often referred as epsilon), (2) minimum number of entries to form a cluster. Time-radius is the maximum time difference that the incoming photons should have to be sorted into the same cluster. If the photons arrive with a time difference that is more than this time-radius, they are sorted into different clusters. For our implementation, the time-radius is 1 nanosecond (2 time slices in the units of 500ps).

For a better understanding of what we call multiplicity, some pictorial examples are shown in the figure 1 and table 1(each histogram is for only one-pixel). We do four tests with our algorithm, and supply it with four scenarios (test-A to test-D) for a single pixel. The result of the clustering that our algorithm performs is expressed in table 1.
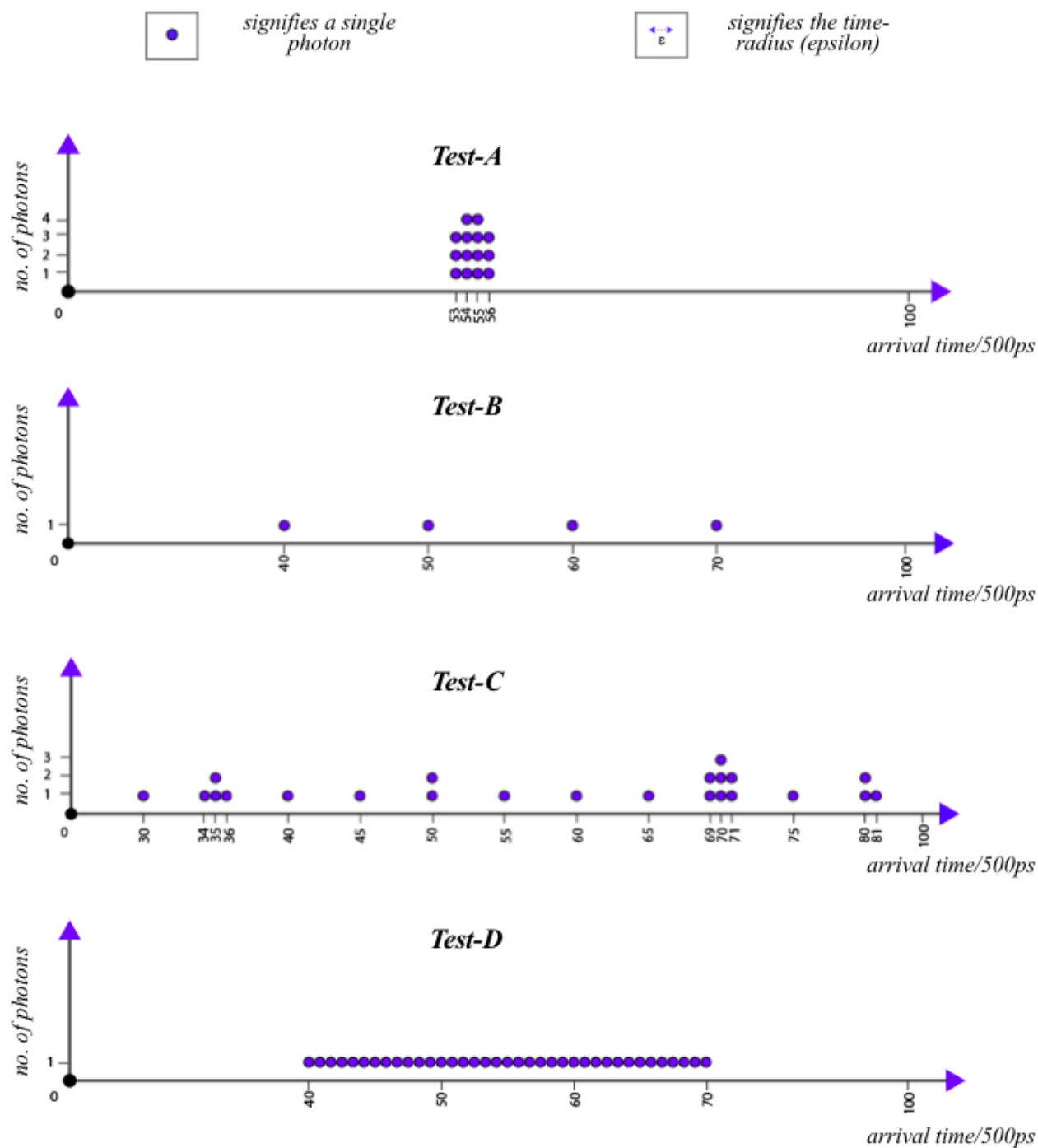
Figure 1 : Histograms showing photons arriving in different time structures.

Test-A	
No. Of photons (multiplicity)	No. Of occurrences/no. of clusters
1	0
....	0
13	0
14	1
15	0
16	0
....	0

Test-B	
No. Of photons (multiplicity)	No. Of occurrences/no. of clusters
1	4
2	0
3	0
4	0
5	0
6	0
....	0

Test-C	
No. Of photons (multiplicity)	No. Of occurrences/no. of clusters
1	7
2	1
3	1
4	1
5	0
6	0
7	1

Test-D	
No. Of photons (multiplicity)	No. Of occurrences/no. of clusters
1	0
....	0
35	0
36	0
37	1
38	0
....	0

Table 1: Test results showing photons arriving in different time structures.

In test-A, we supply the algorithm with single photons that come in a bunch. First, three photons arrive simultaneously, they are sorted into a cluster. Then four photons arrive simultaneously within the time-radius, so they are also sorted in the same cluster. Now, four more photons arrive simultaneously. In this case the time-radius will be taken from the last arriving photon, i.e., the four photons that arrived previously, and not the three photons which came first. So, since these photons arrive within the time-radius from the last four simultaneous photons, they are also sorted in the same cluster. The next three photons also follow this sorting principle, and get sorted in the same cluster. As is clearly seen in the table for test-A, all the number of occurrences are zero, except for the one corresponding to a multiplicity of 14, which has the number of occurrences as 1.

In test-B, we supply the algorithm with single photons that arrive with time difference more than the time-radius. So they are sorted into different clusters. And that is seen in the table for test-B, where all the number of occurrences are zero except for the one corresponding to a multiplicity of 1, which has the number of occurrences as 4.

In test-C, we supply the algorithm with single photons, which arrive in different combinations. All the photons that arrive within the time-radius are sorted into the

same cluster, and the ones arriving later are sorted into a different cluster. This can be seen in the table for test-C.

In test-D, we supply the algorithm with single photons, which arrive continuously and are all within the time-radius of the previous photon. This case is unexpected to happen, because physically this means that a intense photon source is constantly shining on one pixel of the telescope. Nevertheless, we test it with our algorithm, and since the photons arrive within the time-radius of the previous photon, they are expected to be sorted into the same cluster. Note that although test-A and test-D have a very different arrival-time structure, the DBSCAN algorithm produces the same output as long as the number of photons in the cluster is the same.

To get the rates of the multiplicities from these number of occurrences, we need to divide the number of occurrences by the exposure time.

$$rates(multiplicities) = \frac{no.\ of\ occurences}{exposure\ time}$$

There are different trigger mechanisms in FACT. Some of the events are randomly triggered and are unlikely to contain air shower photons. These events are classified under the 'pedestal' trigger of the telescope. Some of the events are triggered because the telescope found a pattern which is likely to contain air shower photons, and such events are classified under the 'physics' trigger of the telescope.
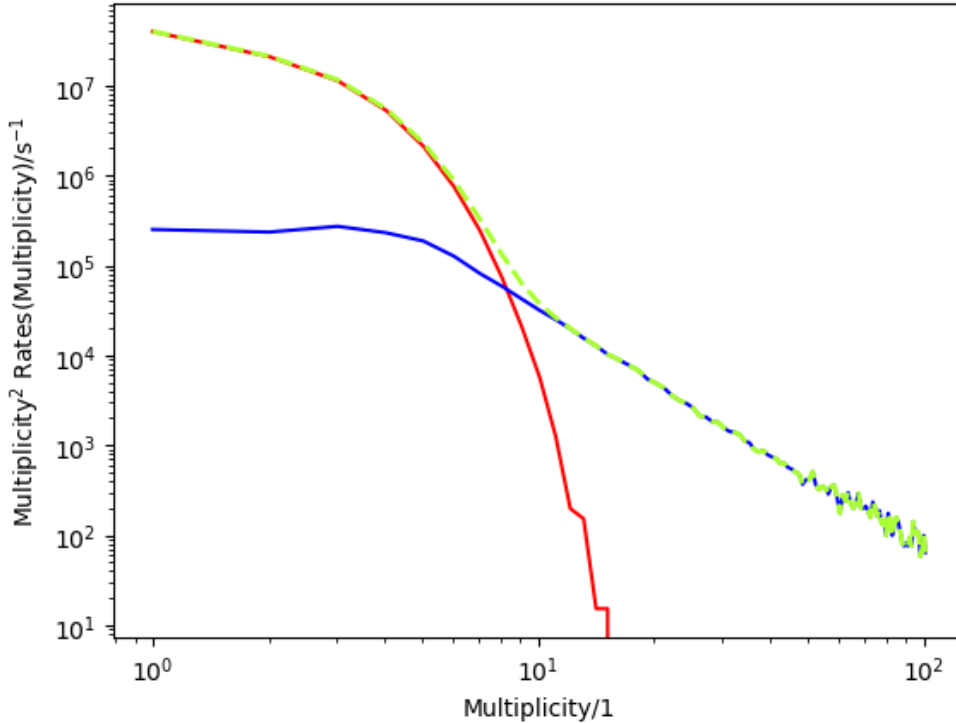

Figure 2: Subtracting the rates of multiplicities of the 'pedestal' trigger events from the rates of multiplicities of the 'physics' trigger events.

The events recorded by the 'pedestal' trigger have the night-sky-background photons, and the events recorded by the 'physics' trigger have both- the night-sky-background photons as well as the air shower photons. To obtain the rates of multiplicities of the air shower photons, we subtract the rates of multiplicities of the 'pedestal' trigger events from the rates of multiplicities of the 'physics' trigger events. Figure 2 shows this same mechanism used in our algorithm. The green curve indicates the 'physics' trigger events, the red curve indicates the 'pedestal' trigger events, and the blue curve indicates the rates of multiplicities of the air shower events that we get after subtracting the rates of multiplicities of the 'pedestal' trigger events (red) from the rates of multiplicities of the 'physics' trigger events (green). So, by using this trigger mechanism, the telescope can statistically differentiate between the air-shower photons and the night sky background photons.

Other works are also going on in the field to monitor the properties of the atmosphere. One such method is LIDAR (Light Imaging, Detection, And Ranging). This method uses laser lights to map the atmosphere, and then make 3D representations of the changes in it. [4][5][6][7]

Results

FACT records a total of 119 auxiliary parameters. Out of these, we selected a few parameters, which, according to us, would have affected the probability of the atmosphere to produce air shower photons the most.
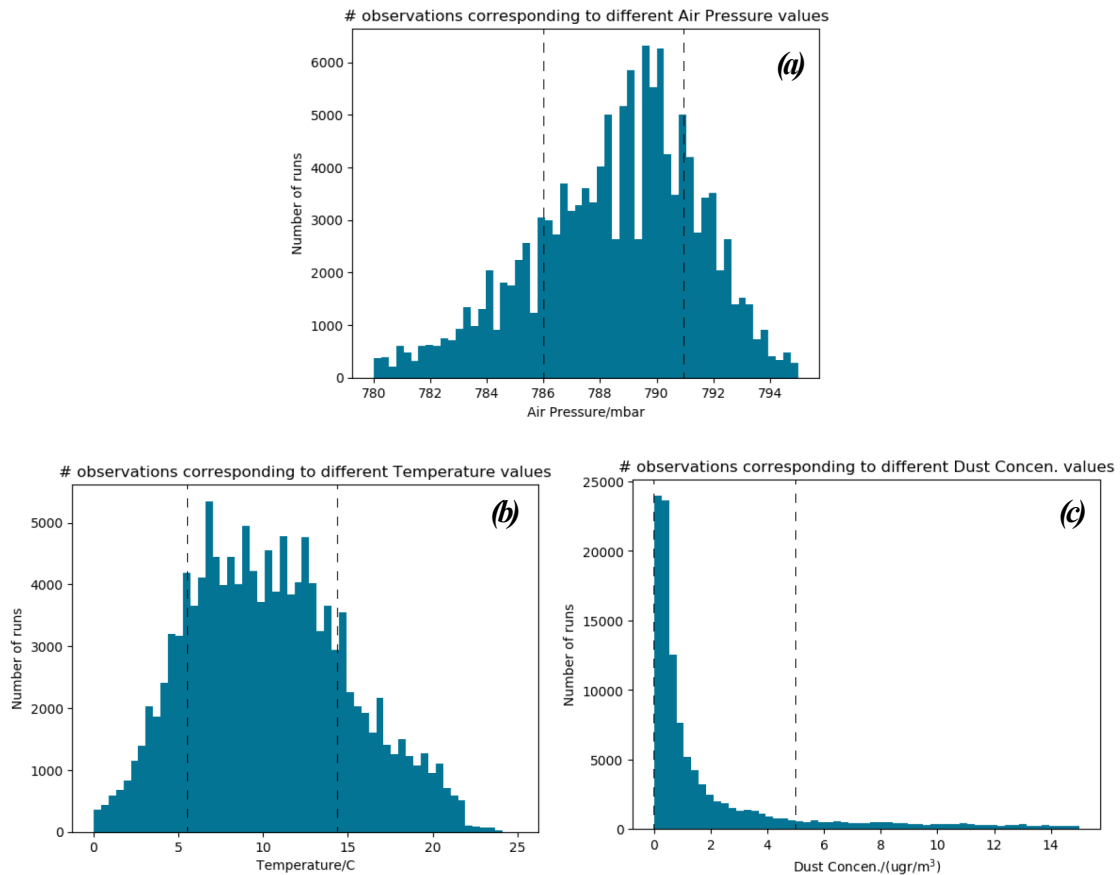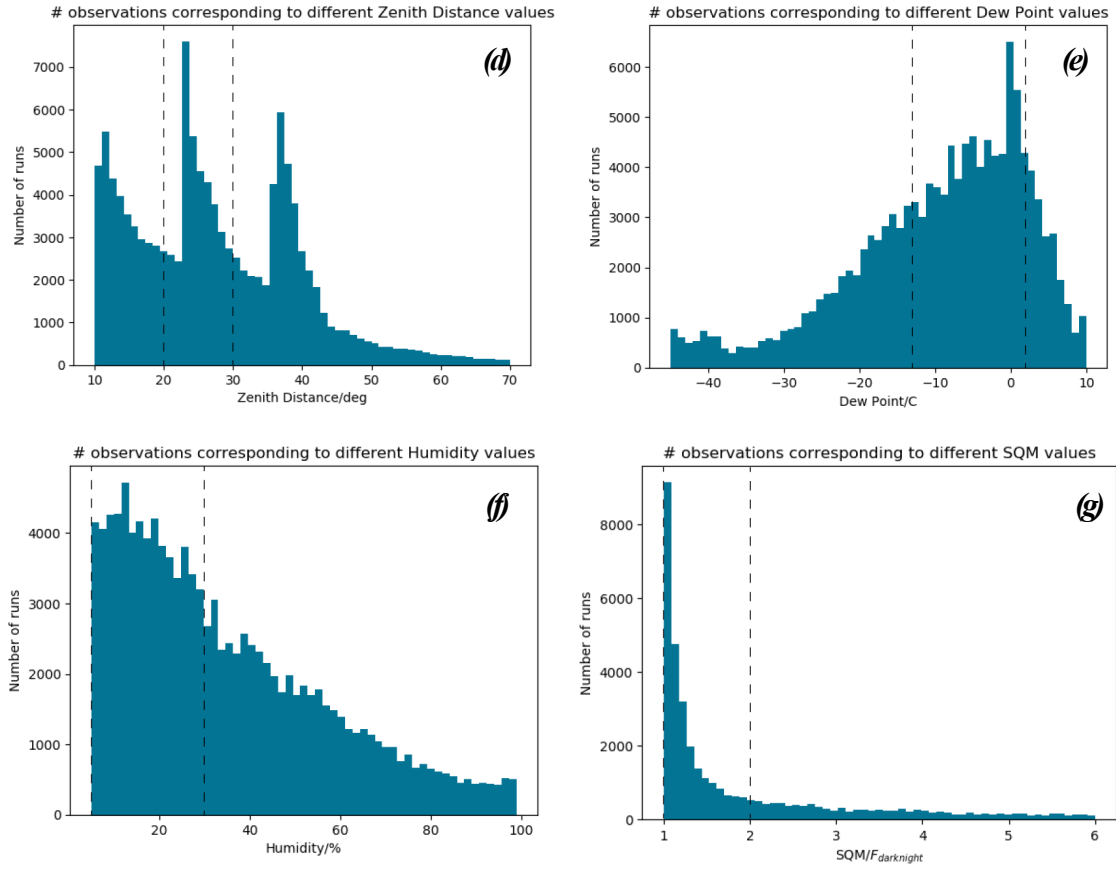
Figure 3

The parameters selected were: air pressure [3(a)], temperature [3(b)], dust concentration in the atmosphere [3(c)], dew point [3(d)], humidity [3(e)], zenith distances of the telescope [3(f)], and the values from the sky quality meter (SQM) [3(g)]. Figure 3 shows the different histograms that give an idea of the number of runs that each parameter has been observed. Since these are atmospheric and ambient properties, one or more of these parameters may be entangled with the rest of the others. So, to minimise any cross correlations whatsoever, we decide a narrow range for each parameter, which is shown using dashed-lines in the histograms for each parameter. We will analyse the plots of one specific quantity, while all the other properties will remain in this specified range. Across this range all the parameters are assumed to be fairly constant, while not compromising with the statistics. This may reduce the probability of cross correlation, and might make the plots less prone to influences from other parameters.

Now, we see the plots for each of these parameters, while all the other parameters are constant in the specified range. The number of statistics that were available for each of the parameters can be seen from the histograms alongside the plots. These plots contain only the air shower multiplicities. It is to be noted that we multiplied the Y-axis of the figures 4 to 10 with multiplicity squared to better highlight the changes in these plots.
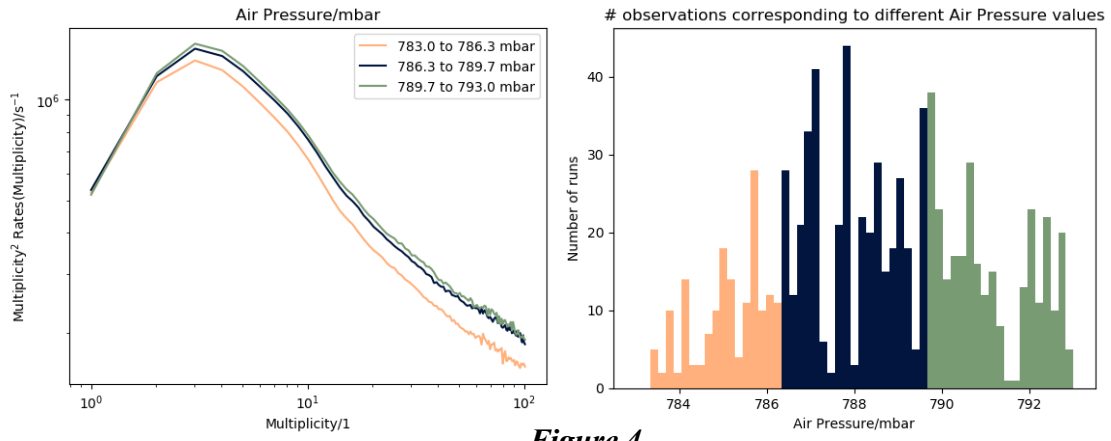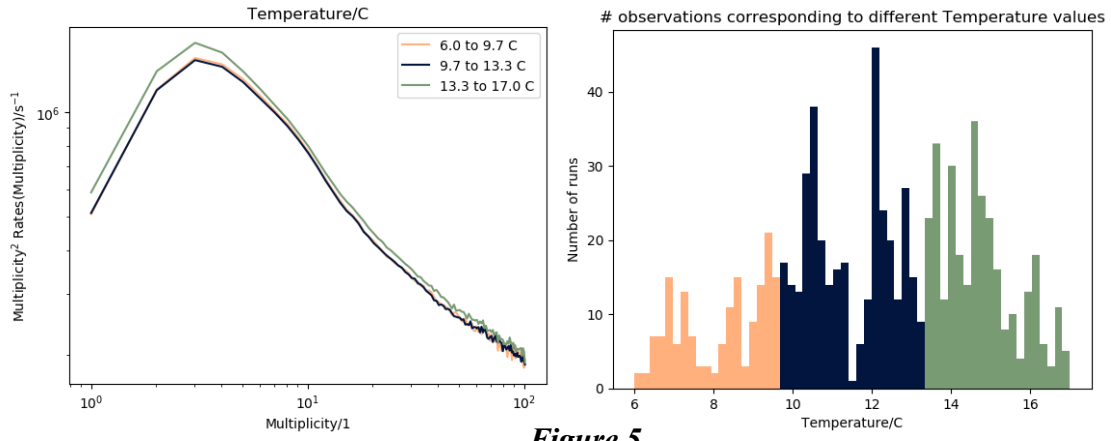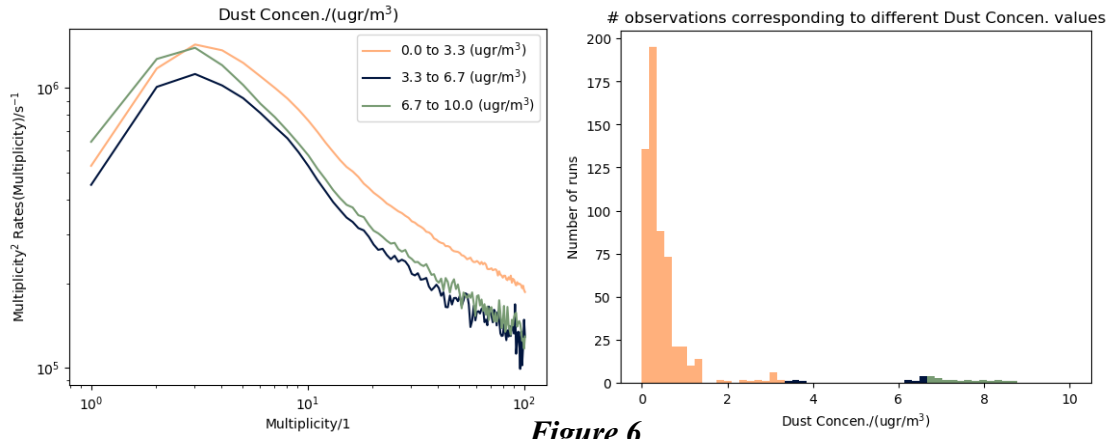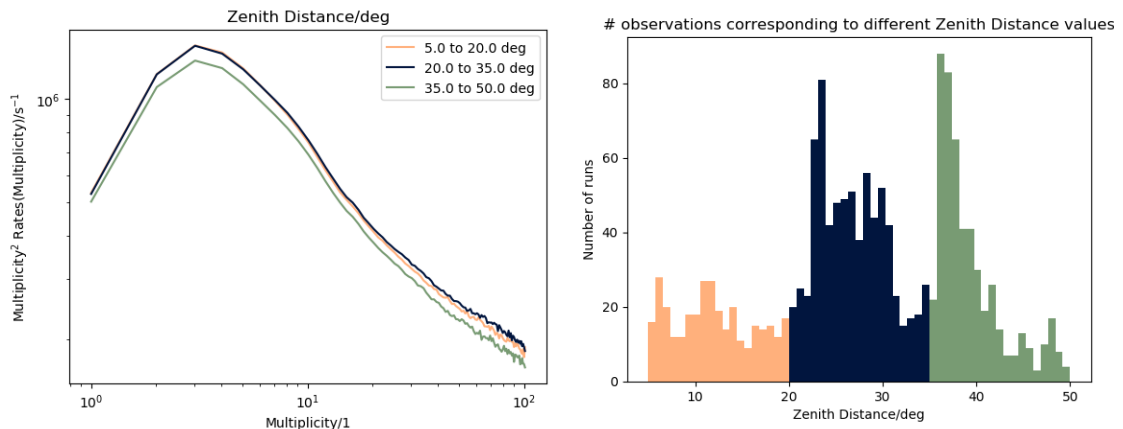
Figure 4

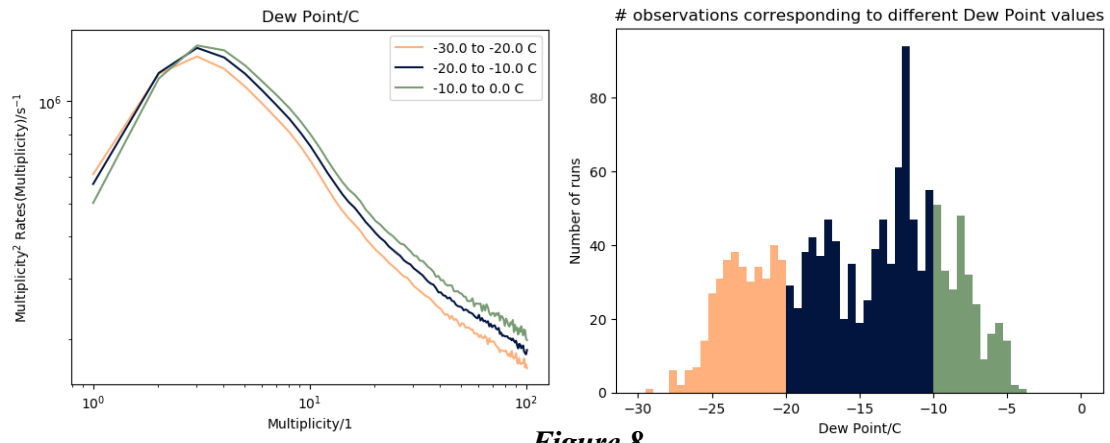## Figure 5
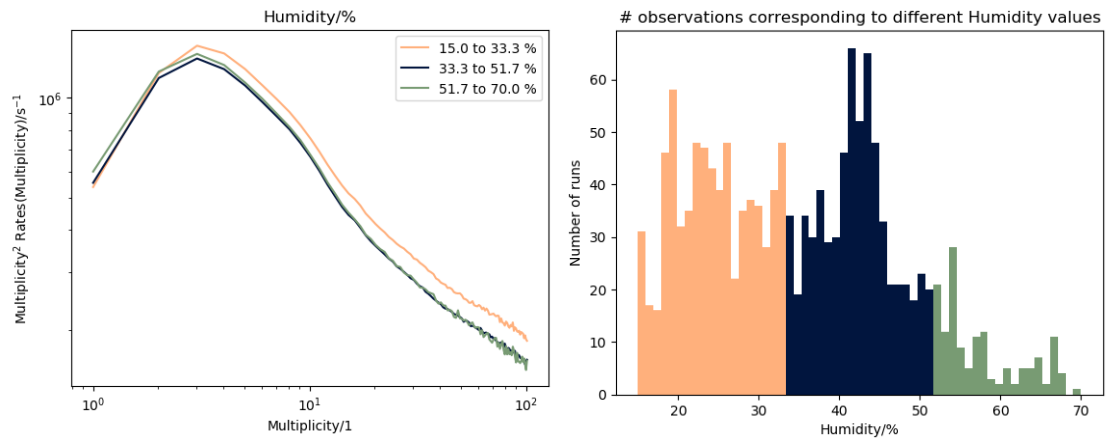

Figure 6
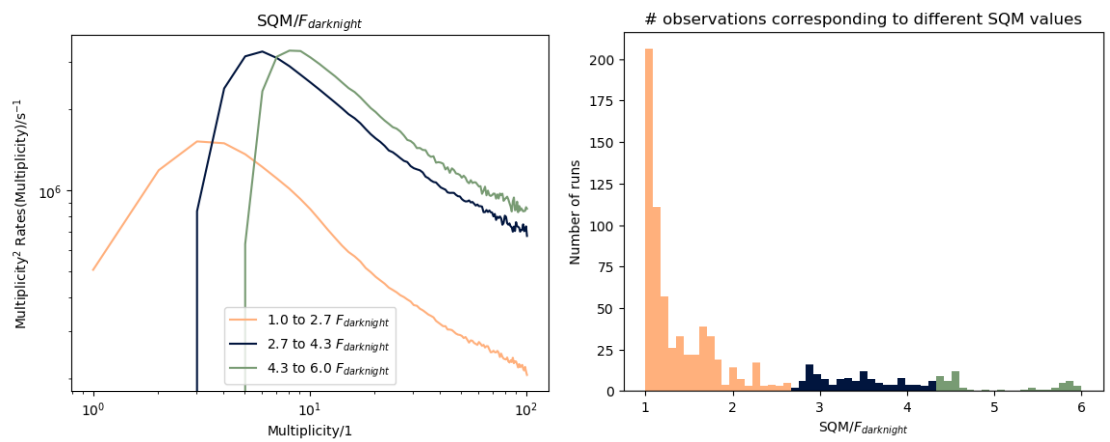

Figure 7

Figure 8

Figure 9

Figure 10

For different air pressures [Figure 4], the rates are almost constant at lower multiplicities. But as the multiplicity increases, the difference in rates becomes more and more apparent, and a pattern starts to emerge. At higher multiplicities, as the pressure increases, the rates also increase.

For different temperatures [Figure 5], we don't observe any correlations with the multiplicity rates.

For different dust concentrations [Figure 6], we observe that there is an effect on the rates, but we cannot say for sure because there is no observable pattern. So, we observe no correlations with the multiplicity rates.

For different zenith distances of the telescope [Figure 7] we don't observe any correlations with the multiplicity rates.

For different dew points [Figure 8], we observe that at lower multiplicities as the dew point increases, the rates decrease. But at a multiplicity of about 4, this pattern is reversed. At higher multiplicities as the dew point increases, the multiplicity rates also increase.

For different humidities [Figure 9], we observe that there is an effect on the rates, but we cannot say for sure because there is no observable pattern. So, we observe no correlations with the multiplicity rates.

For different rates of the night-sky-background photons of the sky quality meter [Figure 10], we observe a correlation with the multiplicity rates. As the flux increases, the multiplicity rates also increase. For multiplicities lower than 9, we see that there are kinks in the plot. This maybe because of how our clustering mechanism works. Incoming single photons are sorted into clusters, but as the photons start arriving more closely, they start getting sorted into a single cluster, and so information of single photons get lost in it. For higher fluxes the trigger threshold increases, and we start observing more and more bright photon clusters.

Conclusions

We observe that the multiplicity rates were clearly affected by some of the atmospheric and ambient properties. For air pressure values, dew points, humidities, and sky quality meter values, we observe a correlation with the multiplicity rates. For dust concentrations, temperature, and zenith distances of the telescope, we observe no correlation with the multiplicity rates.

Further work

From the plots, we saw that there were many small fluctuations, and hence resulted in small random variations in the plots. We suspect that these maybe because of some disturbance in some of the pixels that polluted the overall mean of arrival rates, and hence corrupted the mean data for a run. This lead to small random fluctuations in the plots which might outshine possible correlations with the atmosphere.

This problem might be avoided if we first isolate these corrupted events on a pixel-wise level. This way we may single out all the corrupted events, and exclude them from the mean data for a run. This would require extracting all the telescope data in a format which lists all the arrival rates at different multiplicities in a pixel-wise format. So we will have all the rates for each of the 1440 pixels, for each event. This might help us single out the problematic entries in the data, and also analyse whether these corrupted entries are due to external influences near the telescope, or because of e.g. the power supply for the SiPM pixels of the telescope. Further work might try to analyse the data for each pixel, then isolating the 'bad' entries, and then integrating over all the pixels to combine it into a run that corresponds to the atmospheric and ambient properties.

WWW Availability

The code for this algorithm, the results, and this report can be found on https://github.com/fact-project/runwise_multiplicity .

References and Appendices

[1]: Visible emission of clean liquids by action of γ radiation- Doklady Akademii Nauk SSSR, Vol. 2 (1934), 451 by P. A. Cherenkov

[2]: Design and Operation of FACT -- The First G-APD Cherenkov Telescope, H. Anderhub, M. Backes, A. Biland, V. Boccone, et al. , arXiv: 1304.1710v1

[3]: Single Photon Extraction for FACT's SiPMs allows for Novel IACT Event Representation- S.A. Müller, J. Adam, M.L. Ahnen, D. Baack, M. Balbo, A. Biland, M. Blank, et al., ICRC 2017, Volume 301, 35th International Cosmic Ray Conference, Session Gamma-Ray Astronomy GA-instrumentation, POS(ICRC2017)801

[4]: Lidar: Range-Resolved Optical Remote Sensing of the Atmosphere, by A Weitkamp, C., isbn 9780387251011, lccn 2004052454, Springer Series in Optical Sciences, 2006, Springer New York

[5]: Kam S. Arnold & C. Y. She (2010) Metal fluorescence lidar (light detection and ranging) and the middle atmosphere,Contemporary Physics, 44:1, 35-49, DOI: 10.1080/00107510302713

[6]: Kasparian, J., Rodriquez, M., M'ejean, G., et al. (2003) White-Light Filaments for Atmospheric Analysis. Science, 301, 61-64. http://dx.doi.org/10.1126/science.1085020

[7]: Rairoux, P., Schillinger, H., Niedermeier, S. et al. Appl Phys B (2000) 71: 573. https://doi.org/10.1007/s003400000375

[8]: Ester, M., Kriegel, H.P., Sander, J. and Xu, X., 1996, August. A density-based algorithm for discovering clusters in large spatial databases with noise. In *Kdd* (Vol. 96, No. 34, pp. 226-231).

Acknowledgments

I would like to express my deep gratitude to Professor Dr. Adrian Biland, my project supervisor, for his patient guidance, encouragement and useful critiques of this research work.

I would also like to thank Mr. Sebastian Mueller, for his valuable and constructive suggestions during the planning and development of this project and his assistance in keeping my progress on schedule. His willingness to give his time so generously has been very much appreciated.

I would also like to extend my thanks to the Department of Astrophysics and Astro-Particle Physics for their help in offering me the resources needed for this project.

Finally, I wish to thank my parents and sister for their support and encouragement throughout my study.